

RSC Advances



This is an *Accepted Manuscript*, which has been through the Royal Society of Chemistry peer review process and has been accepted for publication.

Accepted Manuscripts are published online shortly after acceptance, before technical editing, formatting and proof reading. Using this free service, authors can make their results available to the community, in citable form, before we publish the edited article. This *Accepted Manuscript* will be replaced by the edited, formatted and paginated article as soon as this is available.

You can find more information about *Accepted Manuscripts* in the [Information for Authors](#).

Please note that technical editing may introduce minor changes to the text and/or graphics, which may alter content. The journal's standard [Terms & Conditions](#) and the [Ethical guidelines](#) still apply. In no event shall the Royal Society of Chemistry be held responsible for any errors or omissions in this *Accepted Manuscript* or any consequences arising from the use of any information it contains.

Interfacial properties and impact toughness of dendritic hexamethylenetetramine functionalized carbon fiber with varying chain lengths

Lichun Ma^a, Linghui Meng^a, Yuwei Wang^{a,b}, Dapeng Fan^c, Jiali Yu^a, Meiwei Qi^a
Guangshun Wu^a and Yudong Huang^{a*}

^a School of Chemical Engineering and Technology, Harbin Institute of Technology, Harbin 150001, China

^b College of Materials Science and Engineering, Qiqihar University, Qiqihar 161006, China

^c College of Material and Chemical Engineering, Heilongjiang Institute of Technology, Harbin 150001, China

Abstract: In order to understand the effect of chain lengths on the interfacial adhesion of PAN-based carbon fibers (CF) / epoxy composites, dendritic hexamethylenetetramine (HMTA) was functionalized on carbon fibers through quaternary ammonium salt reaction using alkyl dihalide of varying chain lengths $[\text{Cl}(\text{CH}_2)_n\text{Cl}, n = 2, 6 \text{ and } 12]$. Fourier transform infrared spectroscopy (FTIR), Raman spectra and X-ray photoelectron spectroscopy (XPS) confirmed the successful grafting of dendritic HMTA and alkyl dihalide. AFM images showed that dendritic HMTA modified CF surfaces enhanced roughness, and this effect was more pronounced with increasing alkyl dihalide chain length. The results of dynamic contact angle (DCA) and interfacial shear strength (IFSS) demonstrated that the surface energy and interfacial adhesion increased and then decreased with the chain length of alkyl dihalide. The tensile strength and impact roughness of the composites enhanced as the alkyl dihalide chain length grew. Moreover, the reinforcing and toughening mechanisms were also discussed.

Keywords: Carbon fiber; Hexamethylenetetramine; Dendritic; Chain length; Interfacial adhesion.

1. Introduction

Carbon fiber-reinforced composites have become an important foundation of many of today's technologies and structures, in particular in fields like the automotive and aerospace industries, which demand lightweight materials with a high rigidity and strength^{1, 2, 3}. However, applications of fiber reinforced materials are restricted due to the weak interfacial adhesion between fiber and matrix. To satisfy the various technological demands, a sufficient and appropriate interfacial adhesion between fibers and matrix is of crucial importance^{4, 5}. Interfacial adhesion largely depends on molecular interfacial structures and molecular interfacial interactions⁶. Consequently, a variety of surface treatments of carbon fibers are developed such as oxidation, coating,

grafting, and loading, etc.⁷⁻¹². All these surface treatments enhance the interfacial performances by introducing chemically active groups on the fiber surfaces, which increases the reactivity with the matrix, enhancing surface roughness to produce better mechanical interlocking as well as increasing the surface energy for improved wetting¹³.

Though people know the three main effective factors, it is not yet fully understood how these surface treatments ultimately influence the interfacial properties due to the difficulties in quantitatively defining and controlling both the interfacial thickness and chain length on carbon fibers^{13,14}. To further improve and develop advanced composite materials, a solid understanding of interface/interphase concepts is essential^{15,16}. So, it is necessary to look for a proper method that can simplify and model various complicated interfaces to obtain a better insight into the interfacial action mechanisms.

Grafting of polymer or micro-molecule to carbon fiber provides a means to obtain a controlled and ordered structure¹⁷. The grafting method is based on attachment of premade end-functionalized polymer onto the tips and convex walls of the carbon fiber via chemical reactions such as etherification and amidization, or immobilization of reactive groups (initiators) onto the surface, followed by in situ polymerization of appropriate monomers to form polymer grafted carbon fiber. The advantages of this approach are that the mass and distribution of the grafted polymers or micro-molecule can be more precisely controlled and high grafting density can be achieved¹⁸⁻²². In a previous study, we have investigated the chemical grafting approach, which involves the propagation of dendritic hexamethylenetetramine (HMTA) from carbon fiber surfaces by quaternary ammonium salt reaction in the presence of carbon fiber attached haloalkane²³, and dendritic HMTA is a kind of facile and effective coupling agents for increasing the interfacial adhesion of the composites by improving the wettability, enhancing chemical bonding and mechanical interlocking.

Although dendritic molecules are able to improve the interfacial properties between carbon fibers and epoxy matrix, the influence of alkyl chains lengths in the dendritic molecules on the interfacial performance has not been investigated. In this study, we further functionalized dendritic hexamethylenetetramine (HMTA) on carbon fibers through quaternary ammonium salt reaction using alkyl dihalide of varying chain lengths [$\text{Cl}(\text{CH}_2)_n\text{Cl}$, C_n in short, $n = 2, 6$ and 12] to study the effect of chain length of alkyl dihalide on the interfacial adhesion of the composites. In addition, in order to understand the influence of chain lengths on the interface more clearly, we only adopt the second generation dendrimer. Fourier transform infrared spectroscopy (FTIR), Raman spectra and X-ray photoelectron spectroscopy (XPS) were carried out to confirm the alkyl dihalide successful grafting and generation buildup. The wettability of carbon fiber surface was studied by dynamic contact angle analysis (DCA). The effects of chain lengths on mechanical properties of the composites were investigated by micro-bond test, single fiber tensile testing and impact tests. The surface topographies of carbon fiber were observed by atomic force microscopy (AFM) and field emission scanning electron microscope (FESEM).

2. Materials and methods

2.1. Materials

PAN-based carbon fibers (CF), with an average diameter of 7 mm, were purchased from Sino steel Jilin Carbon Co., China. 3-bromo-1-propanol was purchased from Aladdin Co. as reaction intermediate. All other chemicals (acetone, thionyl chloride, dimethyl formamide, pyridine) obtained from Tianjin Bodi Organic Chemicals Co. Ltd. were reagent-grade. Alkyl dihalides which were supplied by J&K Co. are shown in Table.1.

Table.1 Different chain lengths of alkyl dihalides

	Alkyl dihalides	Molecular structure
1	1, 2-dichloroethane	Cl(CH ₂) ₂ Cl
2	1, 6-dichlorohexane	Cl(CH ₂) ₆ Cl
3	1, 12-dichlorododecane	Cl(CH ₂) ₁₂ Cl

2.2. Surface treatment of carbon fiber

The dendritic HMTA grafted CF was prepared through following several steps of chemical reactions. Previous experiments have determined the optimal parameters of the every step of reactions. In brief:

- (i) The CFs were firstly extracted by Soxhlet with acetone in order to remove the polymer sizing and pollutants on the surface of CFs (denoted as untreated CF)²⁴; Second, The CFs were oxidized in AgNO₃/K₂S₂O₈ solution at 343 K for 1 h to introduce polar groups (such as hydroxyl groups, carboxyl groups)²⁵; Subsequently, the CF-COOH was reacted with SOCl₂ for 48 h to yield acyl chloride functionalized CFs (CF-COCl)²⁶⁻²⁹; CF-COCl was reacted with 3-bromo-1-propanol in anhydrous pyridine solution in the ice water bath, and then at room temperature for 3 h to yield CF-Br³⁰⁻³³; Then 0.2g CF-Br was reacted with 0.2g hexamethylenetetramine (HMTA) in 30mL trichloromethane at 333 K for 8 h to produce quaternary ammonium salt reaction and obtained functionalized CF containing the “first generation” amine groups (CF-N⁺Br⁻, CF-G₁-HMTA)^{34, 35}. All reactions were extracted and washed by appropriate solvent. And every reaction step has been worked successfully by XPS²³.
- (ii) The grafting reaction and propagation of dendritic HMTA from the CF surface was accomplished by two processes^{36, 37}: (1) quaternary ammonium salt reaction of alkyl dihalide [Cl(CH₂)_nCl, *n* = 2, 6 and 12] to peripheral amino groups. 0.2g CF-G₁-HMTA was reaction with 20 mL alkyl dihalide [Cl(CH₂)_nCl, *n* = 2, 6 and 12], respectively, the every reaction was maintained at 333 K for 8 h. Following this, carbon fibers were taken out and washed with ethanol for three times, respectively, and then used directly in the next procedure. And (2) quaternary ammonium salt reaction of terminal Cl group by HMTA. The carbon fiber was putted into 30mL trichloromethane, followed by adding 0.2 g HMTA, respectively; the reaction was carried out 333 K for 8 h to obtain the functionalized CF containing the “second generation” amine groups (CF-G_{2(n)}-HMTA, *n*=2, 6 and 12). The resultant was extracted with trichloromethane to remove unreacted HMTA and dried.

A proposed mechanism for grafting dendritic HMTA (CF-G₂-HMTA) onto CF surface by using alkyl dihalide of varying chain lengths is schematically represented below:

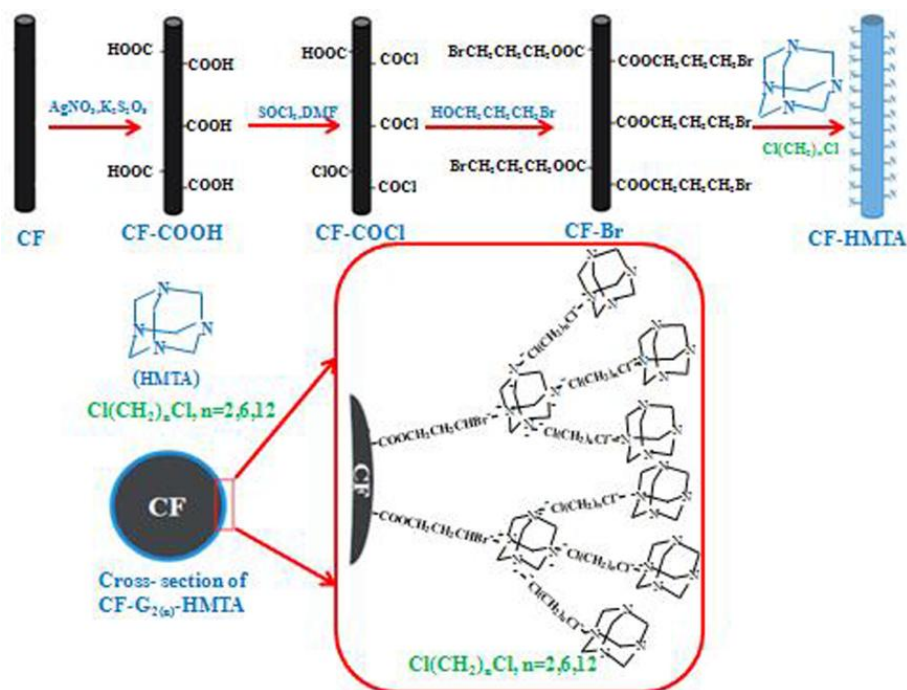


Fig. 1 The schematic of functionalization procedure

2.3. Characterization of carbon fibers

The surface functional groups of the carbon fibers were analyzed by FTIR spectrophotometer (Nicolet, Nexus670, USA). Before the surface analysis, the carbon fiber was dried for 2h under vacuum at 423K. In order to obtain a good optical contact, a very thin KBr layer was introduced between the prism and the carbon fibers by using a KBr pelletizer. The FTIR spectra were acquired by scanning the specimens for 64 times in the wavenumber range of 400-4000 cm^{-1} with the resolution of 2 cm^{-1} .

The surface structures of the carbon fibers were analyzed by Raman spectrometer (Invia Renishaw 2000), the monochromatic light source was an Ar^+ laser (514.5 nm). The laser beam, polarized parallel to the fibers axis, was focused on the samples with the 50 \times objective onto a spot 1~2 μm in diameter, the wavenumber range of Raman spectra was 800-2000 cm^{-1} . The spectra acquired from experiment were analyzed using a Lorentzian curve fitting with a linear baseline to determine the peak areas in the software of WIRE3.3.

XPS (ESCALAB 220i-XL, VG, UK) was carried out to study grafting reaction procedure using a monochromated Al K α source (1486.6 eV) at a base pressure of 2×10^{-9} mbar. The XPS was energy referenced to the C1s peak at 284.6 eV. The XPS peak version 4.1 program was used for data analysis.

Dynamic contact angle tests were measured by using a dynamic contact angle meter and tensiometer (DCAT21, Data Physics Instruments, Germany). Deionised water ($\gamma^d = 21.8 \text{ mN m}^{-1}$, $\gamma = 72.8 \text{ mN m}^{-1}$) and diiodomethane ($\gamma^d = 50.8 \text{ mN m}^{-1}$, $\gamma = 50.8 \text{ mN m}^{-1}$, 99% purity, Alfa Aesar, USA) were used as test liquids. The dispersive and polar

components can be easily determined by solving the following equation:

$$\gamma_1(1 + \cos \theta) = 2(\gamma_1^p \gamma_f^p)^{1/2} + 2(\gamma_1^d \gamma_f^d)^{1/2} \quad (1)$$

$$\gamma_f = \gamma_f^p + \gamma_f^d \quad (2)$$

Where γ_1 , γ_1^d and γ_1^p are the surface tension of immersion liquid, its dispersive and polar component, respectively. Each measurement was repeated three times and the results were averaged.

The interfacial shear strength (IFSS) was adopted to quantify the interfacial property between CFs and resin matrix by the interfacial evaluation equipment (FA620, Japan). The epoxy resin (E-51) and curing agent (H-256) were mixed at the weight ratio of 100:32 to prepare microdroplets. The microdroplets were cured at 363 K for 2 h, 393 K for 2 h and 423 K for 3 h. The values of IFSS were calculated according to equation (3),

$$IFSS = \frac{F}{\pi dl} \quad (3)$$

Where F is the maximum load recorded, d is the carbon fiber diameter, and l is the embedded length. The recorded value of IFSS for each group of specimens was averaged from the data of 80 successful measurements.

Single fiber tensile tests were performed on a universal testing machine (5569, Instron, USA) according to the ASTM D3379-75. The distance between the papers, i.e. the gauge length, was 20 mm. The samples were fixed and tested by the Instron at a cross-head speed of 1 mm min⁻¹. At least 100 samples were tested for CF, the grafted CFs. The results were analyzed with Wellbull statistical method.

The surface topography and roughness of samples before and after being treated was examined by atomic force microscope (AFM, NT-MDT Co., Zelenograd Research Institute of Physical Problems, Moscow, Russia). The observed area was 4 mm × 4 mm. Images were obtained in non-contact mode with a silicon cantilever (nominal spring constant of 3 N/m, minimum tip radius of 10 nm). Each datum was obtained from the average value of 15 different positions on three different fibers.

The unidirectional prepreg of carbon fibers and epoxy resin was put into a mold to manufacture composites. The resin content of the composites was controlled at 35 ± 1.5 mass%. The curing process was at 363 K for 2 h under 5 MPa, 393 K for 2 h under 10 MPa and 423 K for 4 h under 10 MPa.

Impact tests were carried out on a drop weight impact test system (9250HV, Instron, USA). The specimen dimensions were 55 mm × 6.5 mm × 2 mm. The impact span is 40 mm. The drop weight was 3 kg and the velocity was 1 m · s⁻¹. Each date was obtained from the average value of 5 specimens.

The morphologies of the CF, and the grafted CFs after de-bonded and impacted were observed by FESEM (Quanta 200FEG, Hitachi Instrument, Inc. Japan). The samples were coated with a thin conducted gold layer by sputtering prior to the FESEM observation in order to capture a stable and clear image.

3. Results and discussion

3.1 Surface elements and groups analysis of carbon fiber

FTIR is a sensitive technique for surface functional group analysis of carbon fibers³⁸. Fig. 2 shows the FTIR spectra of the untreated CF, CF-G₁-HMTA and three different chain lengths (C₂, C₆ and C₁₂) of CF-G₂-HMTA. For the untreated fibers, in addition to the bonds of the adsorbed water on the fiber surface and carbon dioxide in the air, there are some organic groups that can be observed. The broad band centered at about 3600-3100cm⁻¹ corresponds to the combination of O-H stretching vibration, the bands in the range of 1059-1099cm⁻¹ and 2980-2800 cm⁻¹ are assigned to the C-C and C-H stretching vibration, respectively. For the HMTA grafted carbon fiber, many new bands were obviously detected, a new absorption peak at 1700cm⁻¹ which is attributed to the C=O stretching modes of carbonyl group on the carbon fiber generated by the oxidized treatment, the broad band at 1020-1500cm⁻¹ is assigned to the stretching vibration of the C-N bond³⁹, indicating the HMTA was grafted to the carbon fiber surface through chemical bonds. For the CF-G₂-HMTA, the peaks at 1020-1500cm⁻¹ are progressively stronger, indicating the presence of increasing amount of HMTA with the dendritic generation number. In the spectras of the CF-G_{2(n)}-HMTA ($n = 2, 6$ and 12), the intensity of C-C and C-H bond enhance as the chain lengths of alkyl dihalide increase, indicating the alkyl dihalide was grafted to the carbon fiber surface through chemical bonds.

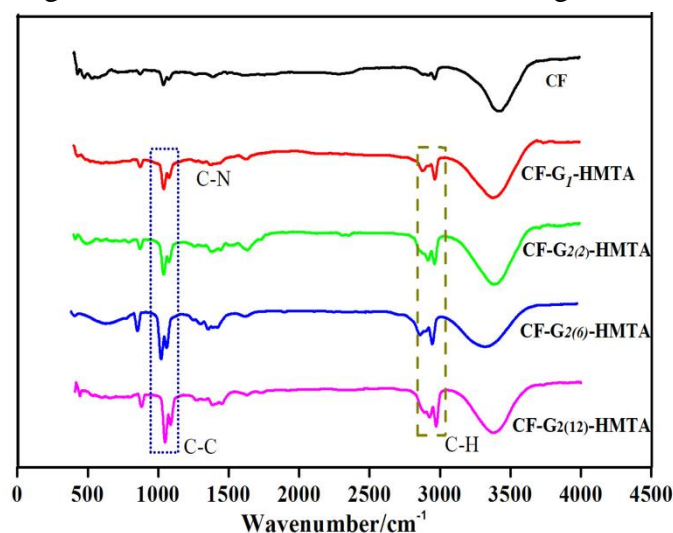


Fig.2 FTIR spectra of untreated CF, CF-G₁-HMTA and CF-G_{2(n)}-HMTA ($n=2, 6$ and 12)

To further analyze the surface structures of the CF and grafted CFs, Raman spectroscopy was adopted. The Raman spectra of carbonaceous materials have two characteristic bands including: (1) “D-band”, centered at the wavenumber of 1330-1350cm⁻¹ that is attributed to defects and disordered carbonaceous structure, and (2) “G-band”, located at the wavenumber of 1580-1600cm⁻¹ that is related to ordered graphitic structures. The integral area ratio of the “D-band” to the “G-band” (I_D/I_G , known as the “R-value”) indicates the amount of structurally ordered graphite crystallites in the carbonaceous materials⁴⁰.

In addition, the overlap between D and G peak is serious, which is not conducive to

analyze thoroughly, therefore, the spectra must be fitted. “A-band” around $1500\text{-}1550\text{cm}^{-1}$ has been observed in some carbon materials with lower ordered structure (such as glassy carbon, carbon black and so on), it is associated with amorphous carbonaceous structures, some hetero atoms on the surfaces of CFs or some original functional groups⁴¹⁻⁴³. The integral area ratio of the “A-band” to the “G band” (I_A/I_G) indicates the proportion of amorphous carbonaceous structures as well as some oxygen-containing and/or nitrogen containing functional groups on the CFs surface.

The Raman spectra and curve fitting using the Lorentzian-Gaussian method with the software of WIRE3.3 for untreated CF, CF-G₁-HMTA, and CF-G_{2(n)}-HMTA ($n = 2, 6$ and 12) are shown in Fig. 3. The wave numbers of three bands and the calculated values of “ I_D/I_G ” and “ I_A/I_G ” are shown in Table. 2. It indicated that the micro-structure of carbon fibers surface changed after grafting.

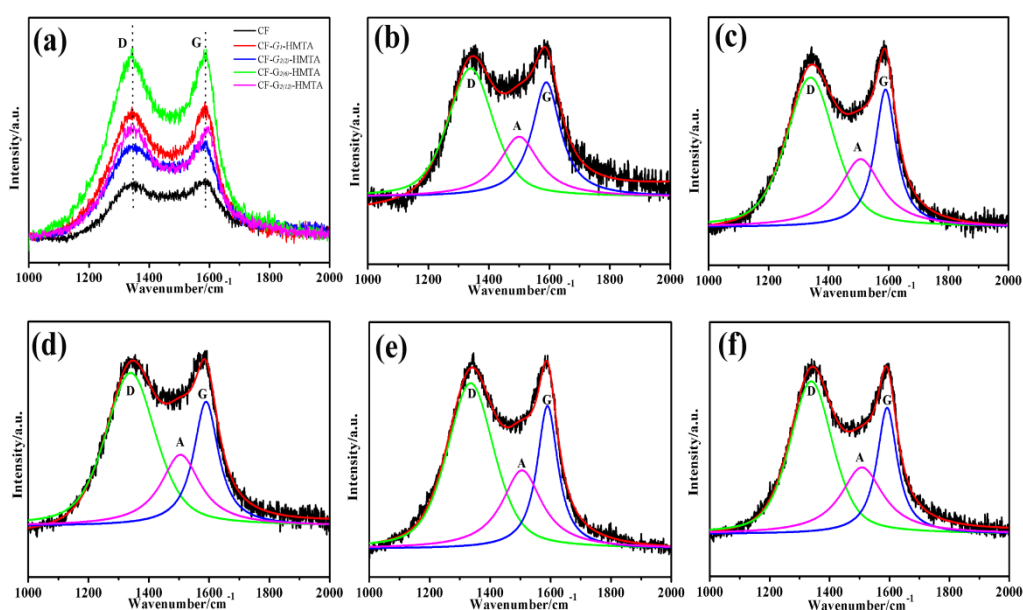


Fig.3 Raman spectra (a) and curve fitting for all the samples (b) CF, (c) CF-G₁-HMTA, (d, e, f) CF-G_{2(n)}-HMTA ($n=2,6$ and 12)

Table.2 Wavenumbers of D, G and A bands and the calculated values of “ I_D/I_G ” and “ I_A/I_G ” acquired from CFs

Samples	D	G	A	$R=I_D/I_G$	I_A/I_G
	W(cm^{-1})	W(cm^{-1})	W(cm^{-1})		
CF	1340	1590	1500	1.46	0.69
CF-G ₁ -HMTA	1340	1590	1508	2.05	0.87
CF-G ₂₍₂₎ -HMTA	1340	1590	1505	2.06	0.93
CF-G ₂₍₆₎ -HMTA	1336	1590	1505	2.03	1.06
CF-G ₂₍₁₂₎ -HMTA	1339	1592	1508	2.02	1.11

Compared to the untreated CF, the “R (I_D/I_G)” value of CFs after being grafted HMTA (CF-G₁-HMTA) increased to 2.05 from 1.46, which indicated that the oxidation in the process of grafting partially damaged the structurally ordered sheath region of

CFs, a suitable etching would preferably remove the carbonaceous structures on the fiber surface, the disordered carbonaceous components on the surface of CFs was improved, and the crystalline structure of the CFs was reduced. And as the dendritic generation and chain lengths increased, the “ $R(I_D/I_G)$ ” values were slightly affected.

However, “ I_A/I_G ” value of the CF after being grafted HMTA increased significantly, from 0.69 for un-treated CF to 0.87 for CF- G_1 -HMTA, which proved that the amorphous carbonaceous structures(C-C, C-H bond) as well as nitrogen-containing functional groups (HMTA) were grafted on the surface of CFs, and the “ I_A/I_G ” values gradually increased as the dendritic generation and chain lengths increased, which would mean that the more nitrogen-containing functional groups will provide more activity sites to improve the interfacial strength of the composites.

XPS is a very sensitive and surface specific analytical tool. To further present enough evidence of HMTA and alkyl dihalide grafted onto carbon fiber surface, we used high-resolution XPS to detect the surface composition and the chemical environment of CF- $G_{2(n)}$ -HMTA($n = 2, 6$ and 12), The survey spectrum of CFs and C1s peak positions derived from peak deconvolution and fitting to data are listed in Fig. 4 and Table 3. The XPS C1s core-level spectrum of untreated CF (Fig. 4a) was resolved into three component peaks: Csp^2 and Csp^3 in the fiber structure (peak C1s (1), 284.4 eV), C-C bonding of amorphous carbon (peak C1s (2), 285.6 eV) and C-O bond (peak C1s (3), 286.3 eV)⁴⁴⁻⁴⁶, As shown in Table 3, the content is 74.5%, 18.44%, 7.06%, respectively. The C1s peak of CF- G_1 -HMTA (Fig. 4b) shows a peak assigned to $-C=O$ (C1s (4), 287.3 eV) generated on the CF through $AgNO_3/K_2S_2O_8$ oxidation. What's more, there were two additional binding energy peaks at 286.3 eV and 285.8 eV, which is assigned to new generated bond $C-N^+$ by quaternary ammonium salt reaction and C-N bond existence in the HMTA^{47,48}, and the content of C-N and $C-N^+$ bond increased with the dendritic generation number as shown in Table 3. These amine groups grafted onto the fiber surface would effectively increase the polarity of the carbon fiber surface and make the fibers more easily further react with epoxy matrix and enhance the interfacial strength of the composites. In addition, compare the CF- $G_{2(n)}$ -HMTA($n=2, 6$ and 12), as the chain lengths of alkyl dihalide increased, the peak areas of C-C (peak C1s(1) 284.4 eV) increased, indicating the alkyl dihalide has been grafted to the HMTA through quaternary ammonium salt reaction, which was consistent with the results of the FTIR discussed above. Moreover, the content of C-N and $C-N^+$ increased, this is due to the growth of molecular chain, the steric hindrance effect between rigid HMTAs reduced, thereby more HMTA molecules could be grafted to alkyl dihalide. While as $n=12$, the content of C-N and $C-N^+$ decreased, this is possibly because that the long chain alkyl dihalide has good flexibility, molecular chain curls and wraps the polar functional groups from being exposed outside, and the G_2 -HMTA can not be grafted, which lead to the content of C-N and $C-N^+$ decreased. From the survey spectrum of CFs, we also found that the content of nitrogen element (N1s, 400.5 eV) increased greatly and then decreased.

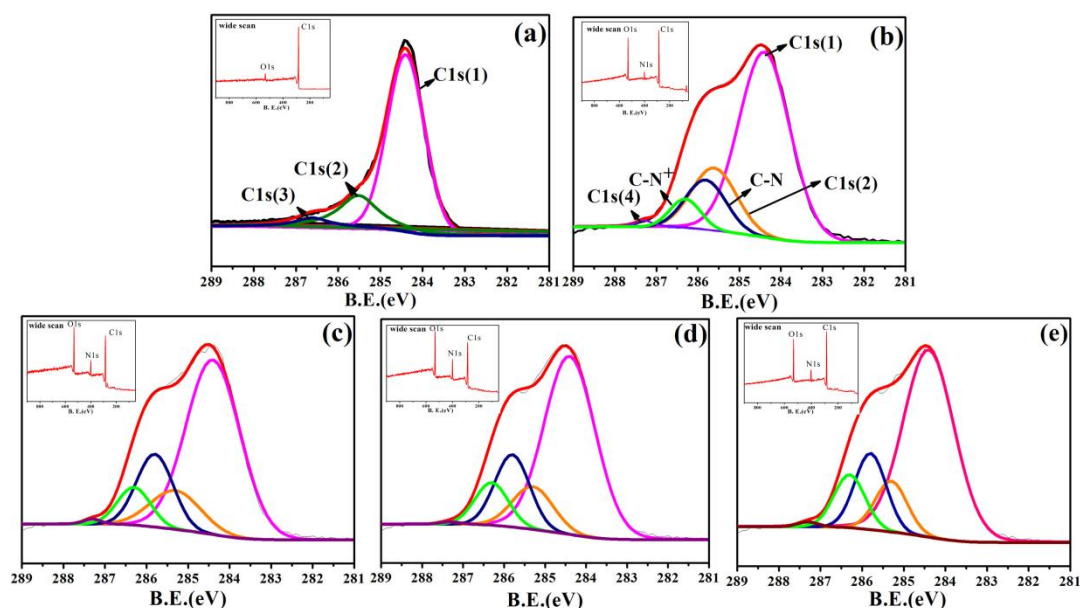


Fig.4 XPS survey spectrum and curve fitting for C1s peak (a) CF, (b) CF-G₁-HMTA, (c, d, e) CF-G_{2(n)}-HMTA (n=2,6 and 12)

Table.3 Surface groups analysis of the carbon fibers

Samples	The relative content of functional group (%)				
	C1s (1)	C1s (2)	C1s (3)	C1s (4)	C1s (5)
	C-C	C-C/C-N/C-N ⁺	C-O	C=O	-COOH
CF	74.50	18.44 - / -	7.06	-	-
CF-G ₁ -HMTA	67.50	10.00 / 12.85 / 4.05	-	5.60	-
CF-G ₂₍₂₎ -HMTA	61.52	10.59/17.19/8.03	-	2.67	-
CF-G ₂₍₆₎ -HMTA	63.26	7.99/16.93/10.51	-	1.31	-
CF-G ₂₍₁₂₎ -HMTA	65.20	9.41/15.25/9.52	-	0.62	-

In short, through the analysis of FTIR, Raman and XPS, it could be concluded that alkyl dihalide and dendritic HMTA are well organized and grafted to the CF surfaces.

3.2 Surface topography of carbon fibers

The 3D topographies of CF and treated CFs surfaces were examined by AFM in Fig. 5. And the corresponding surface roughness, Ra, derived from the AFM scans were also listed in Fig. 5. This Ra value is an arithmetic average of the absolute values of the surface height deviations measured from the best fitting plane⁴⁹. The untreated carbon fiber (Fig. 5a) presents a similarly smooth surface and a few narrow grooves parallel distribute along the longitudinal direction of the fiber, which is due to the fiber manufacture process. Compared with the surface of untreated CF, the fiber surface roughness (Ra) of CF-G₁-HMTA obviously increases, from 14.6 nm to 35.4nm (Fig. 5b), the HMTA are grafted and distribute uniformly on the CF at different directions and

increase the polarity of CF surface. As the dendritic generation increases (Fig. 5c), the fiber surface roughness greatly increases, which means that more HMTA were grafted on to the CF surface. In addition, compared the topographies of CF-G_{2(n)}-HMTA ($n = 2, 6$ and 12) in Fig. 5(c, d, e), it can be observed that as the chain lengths of alkyl dihalide increased, the peak diffused on surface of CF was higher and higher. The Ra increased from 48.7 nm for CF-G₂₍₂₎-HMTA to 82.3 nm for CF-G₂₍₁₂₎-HMTA, the finding are in good agreement with Duchet et al, who suggested that the toughness can be improved by the presence of tethered chains at the interface⁵⁰. The increased roughness can provide more contact points and enhance the mechanical interlocking between the fiber and the matrix, thus improve the interfacial adhesion of the resulting composites.

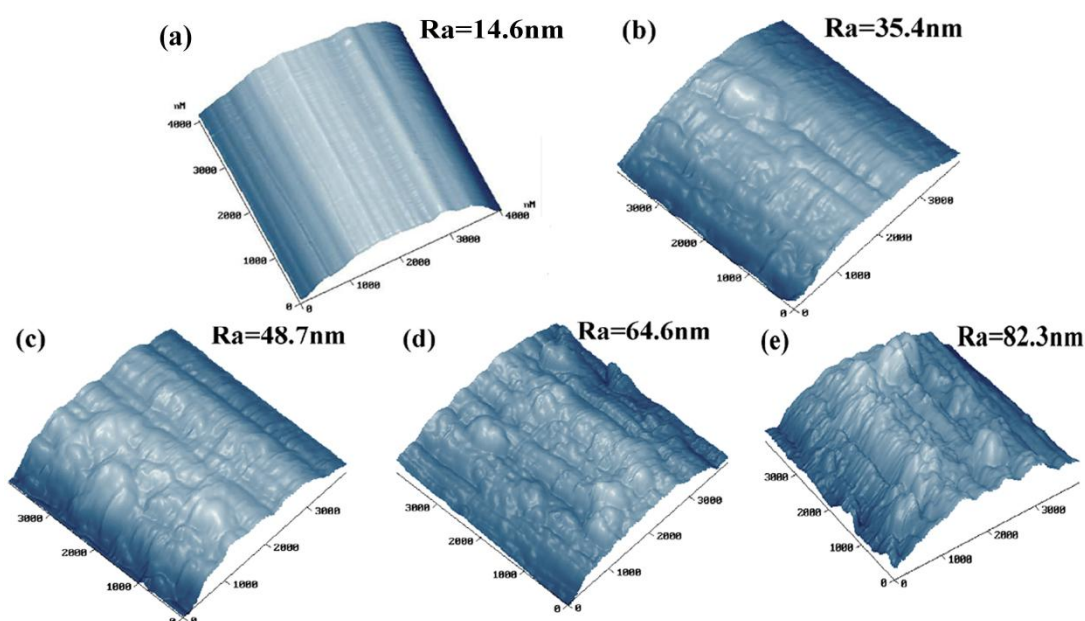


Fig.5 3D AFM images of CF surface: (a) untreated, (b) CF-G₁- HMTA, (c, d, e) CF-G_{2(n)}- HMTA ($n=2, 6$ and 12)

3.3. Dynamic contact angle analysis

The increase of the fiber surface energy could lead to better wettability between carbon fibers and matrix, and improve the interface adhesion^{51, 52}. The surface free energy consists of two components: dispersive component (γ^d) and polar component (γ^p), which are determined by the contact angle based on the dynamic contact angle of double fluid methods. The testing liquids used are water and diiodomethane, whose surface energies are known, the dispersive and polar components can be easily determined by solving the Eq. (1). In Fig.6, the advancing contact angle (θ), the surface energy (γ), its dispersion component (γ^d) and polar component (γ^p) of the untreated CF, CF-G₁-HMTA, and CF-G_{2(n)}-HMTA ($n = 2, 6$ and 12) are summarized. As shown in Fig.6, the surface free energy shows an obvious increase after the grafting of HMTA and G₂-HMTA onto CF in comparison with untreated CF.

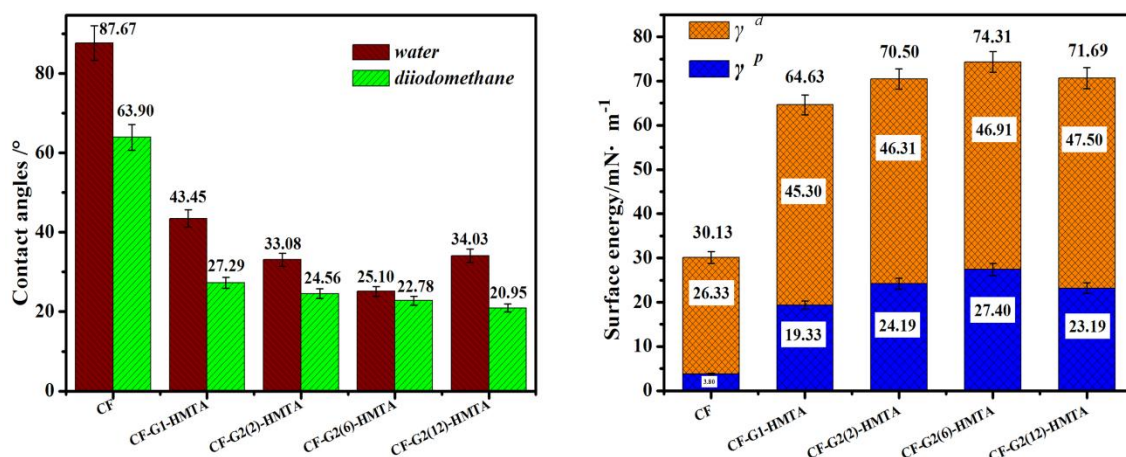


Fig.6 Contact angles and surface energy of untreated CF, CF-G₁-HMTA and CF-G_{2(n)}-HMTA ($n=2, 6$ and 12)

Compare the CF-G_{2(n)}-HMTA ($n = 2, 6$ and 12), as $n=6$, the contact angles decreased from 33.08 to 25.10° for water and from 24.56 to 22.78° for diiodomethane. The increased polar component of surface energy could be interpreted by the increase of amine groups caused by more HMTA grafted on the fiber surface. In addition, the increased dispersion component could be attributed to the increased fiber surface roughness caused by the longer chain of alkyl dihalide, so both the dispersion component (γ^d) and polar component (γ^p) make it have the highest surface energy. As $n=12$, the contact angle increased for water, this could also be due to the fact that the long alkyl dihalide chain curls and blocks the polar functional groups from being exposed on the entire system surface, which lead to the reduction of polar groups. But the contact angle still decrease for diiodomethane as the growth of carbon chain. Owing to the extent of increment of dispersive component is higher than the extent of decrement of polar component, the CF-G₂₍₁₂₎-HMTA which has the highest dispersion component owns the higher surface energy compared CF-G₂₍₂₎-HMTA and lower surface energy compared CF-G₂₍₆₎-HMTA. In short, the higher surface energy could lead to a better wettability especially for the polar matrices, which is beneficial to the subsequent formation of covalent bonding, van der Waals interaction and physical entanglement, and could greatly enhance the interfacial properties of composites.

3.4. Interfacial property testing

The interfacial strength of the composites was evaluated by single fiber pull-out tests. Fig.7 shows the interfacial shear strength (IFSS) results of CF, CF-G₁-HMTA and CF-G_{2(n)}-HMTA ($n = 2, 6$ and 12). The results indicate that grafting HMTA on CF surface improved the interfacial adhesion of fiber/epoxy composite significantly. The IFSS of CF-G₁-HMTA and CF-G₂₍₂₎-HMTA composites are increased by 61.02% and 70.72% compared to untreated composite. We attribute the high interfacial mechanical properties enhancement to the fact that the number of grafted amine functional groups increased with dendritic generation, the dendritic peripheral tertiary amino groups can react with epoxy groups through anionic polymerization, which improves stress transfer

between CF and the epoxy resin, therefore, the IFSS greatly improved with the dendritic generation number.

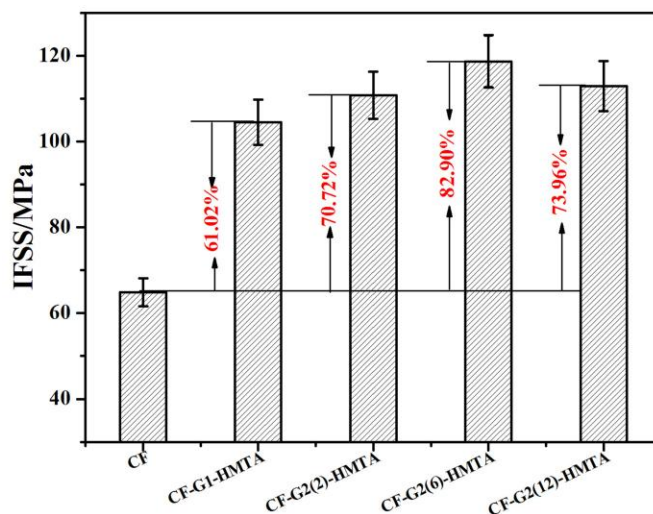


Fig. 7 Interfacial shear strength (IFSS) of the composites

Furthermore, after the carbon chain (C_2) of CF- $G_{2(2)}$ -HMTA surfaces were replaced with C_6 , the composite also showed significant improvement in IFSS, improved by 82.90% compared to untreated composite, at the same time, the value of IFSS is also higher than that of CF- G_3 -HMTA obtained in previous study²³. This may be because the longer alkyl chain in CF- $G_{2(6)}$ -HMTA make the distance between HMTAs of generation 1 and 2 increase, and the steric hindrance effect of rigid molecules reduced, thereby more HMTA molecules could be easily grafted to alkyl dihalide. In addition, there are much broad space in the molecular interior and exterior, epoxy matrix can infiltrate into molecular interior and exterior to form a strong mechanical interlocking with CF, which result a better adhesion at the interface, therefore the stress transfer more efficiency from the matrix to CF increased.

Whereas the longest alkyl chains of C_{12} , due to the flexibility, it is easily to curl and block a part of polar functional groups from being exposed on outermost surface, making the G_2 -HMTA can not be grafted. Meanwhile, the end of chains itself may not be able to graft new active group, so the value of IFSS lower. Although polar group has less contribution to the improvement of interfacial properties, the interaction physical entanglement between the long chain and the chain of epoxy at the interface is responsible for the improvement of interfacial performances to some extent, therefore the IFSS value is still higher than CF- $G_{2(2)}$ -HMTA.

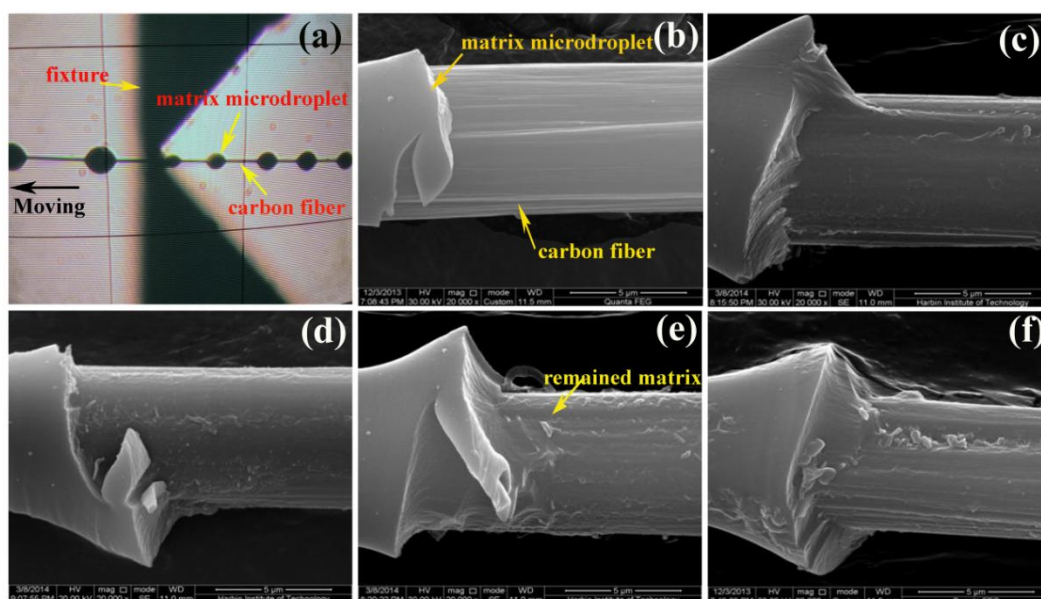


Fig. 8 SEM micrographs of before de-bonding (a) and after de-bonding samples: (b) untreated CF, (c) CF-G₁-HMTA, (d, e, f) CF-G_{2(n)}-HMTA ($n=2, 6$ and 12)

In order to further confirm the reason for such an enhancement, the surface morphologies of CFs de-bonding from the matrix were examined by FESEM, as shown in Fig. 8. In the case of untreated CF, the de-bonded CF surface (Fig. 8b) is almost neat. Scilicet, there is almost no epoxy remained on the CF surface, which indicates that the interface is easily de-bonded due to the weak Van der Waals force reaction between CF and epoxy⁵³. In the case of HMTA functionalized CF, the CF surface (Fig. 8c) is not as smooth as that for the CF-G₁-HMTA, that is to say that some epoxy have remained on the CF surface, which signifies the interface between CF and epoxy becomes so strong that fracture is not restricted to the interface only. As mentioned above, the HMTA not only links to the CF by the chemical interactions, but also reacts with epoxy matrix as curing agent. As a result, the bonding between CF and epoxy is not the Van der Waals interaction but chemical interaction. Fig. 8d presents the surface morphology of CF-G₂₍₂₎-HMTA, the remained epoxy is more than the case of CF-G₁-HMTA, which further conformed that the interfacial performance greatly improved as the growth of dendritic generation.

Compare the surface morphologies of CF-G_{2(n)}-HMTA ($n=2, 6$ and 12) de-bonding from the matrix. It can be seen that the surface CF-G₂₍₆₎-HMTA was almost covered by remained epoxy and the de-bonding took place in the matrix (Fig.8e). In addition to the active functional groups increased, the longer chain of alkyl dihalide grafting must lead to increased roughness of the CF surface, which enhances the mechanical interlocking effect between the CF and matrix. The pullout of CF from the epoxy matrix certainly consumes some more energy thus enhancing the interfacial strength. Fig. 8f presents the surface morphology of CF-G₂₍₁₂₎-HMTA, the remained epoxy is more than the case of CF-G₂₍₂₎-HMTA, but less than the case of CF-G₂₍₆₎-HMTA. The longest chains of alkyl dihalide make the interaction physical entanglement with the chain of epoxy increase, but the active groups which exposed in the outside surface and take part in the chemical

interactions with epoxy matrix may reduce, so remained epoxy is less than the surface of CF-G₂₍₆₎-HMTA. These observations are consistent with the IFSS results. The stronger the interfacial shear strength, the more epoxy remained on the CF surface.

3.5. Single fiber tensile testing

The presence of strong interfacial bonding alone may not always lead to satisfactory overall performance⁵⁴. Single fiber tensile tests are also adopted to examine the effect of the modification and chain lengths on the tensile strength of the fibers, which affects the in-plane properties of the resulting composites. CF is a brittle and high scatter material, single tensile testing results are usually difficult to analyze, so the tensile strength data are often statistically analyzed with Weibull distribution function⁵⁵. The results of the fiber tensile testing are presented in Table.4, it can be seen that the grafting of HMTA on the CF surface led to decrease slightly in fiber tensile strength, but the reduction can be neglected, which means this oxidation and grafting process can effectively protect the fibers from introducing defects and damages on the surface structures of fiber. Moreover, the fiber tensile strength was discovered a little increasing trends from CF-G₁-HMTA to CF-G₂₍₁₂₎-HMTA, from 3.78 GPa to 3.98 GPa, which is due to the fact that the molecular chains grafted onto CF growth as the increasing of dendritic generation and chain length of alkyl dihalide, they could tangle mutually to form similar reticular crosslink structure and protect the CF from preventing to be pulled apart. The results of the single fiber tensile testing imply that increasing the length of molecular chains would increase the in-plane properties of the resulting composites at a certain extent.

Table.4 Single fiber tensile strength of carbon fiber specimens

Sample	Ra	m	Σ_0	Expectation(GPa)
CF	0.99	-4.98	3.91	3.80
CF-G ₁ -HMTA	0.99	-4.96	3.86	3.78
CF-G ₂₍₂₎ -HMTA	0.97	-5.16	3.87	3.83
CF-G ₂₍₆₎ -HMTA	0.99	-5.23	3.88	3.92
CF-G ₂₍₁₂₎ -HMTA	0.98	-5.38	3.96	3.98

3.6. Impact property testing

The impact property tests were carried out to examine the effect of the HMTA and the chain lengths of alkyl dihalide on the impact resistance of the composites. As shown in Fig. 9a, the impact strength of the untreated carbon fiber composites is 55.77kJ/m², the surface of fiber cannot fully contact with matrix resin molecules due to the poor wettability with matrix resin, and there would be many defects in the interface during the manufacture process of composite. In addition, the chemical action between fiber surface and matrix resin is poor because of the lack of active functional groups, so the interfacial adhesion is very weak, when the composites are under a small load, the interface cracks easily occurs. After being grafted with HMTA and G₂-HMTA, the impact strength of the composite obviously increases to 64.56 and 68.90kJ/m², respectively, which could be due to the increase of interface adhesion as discussed

above, and the needing energy to destroy the interface increased. If there is no appropriate interphase, the crack tip extends perpendicular to the fiber surface, which would lead to fiber fracture under low stress. The dendritic interphase worked as a shielding layer which could relieve the stress concentration, prevent the crack tips from directly contacting with the fiber surface and make the crack path deviate away from the fiber surface to the interphase region⁵⁶. In addition, numerous cage-like structure molecule-HMTAs on the fiber interface could induce more cracks when the major crack passed to them, and the communication process become difficult, which could efficiently absorb more fracture energy. Moreover, the flexible long chain length of alkyl dihalide was also beneficial to increase the impact resistance by preventing the crack tip propagation and blunting the crack tip. The longer of the chain length of alkyl dihalide, the more fracture energy would be consumed. Therefore, as the chain length of alkyl dihalide growth, the impact strength of composites enhanced.

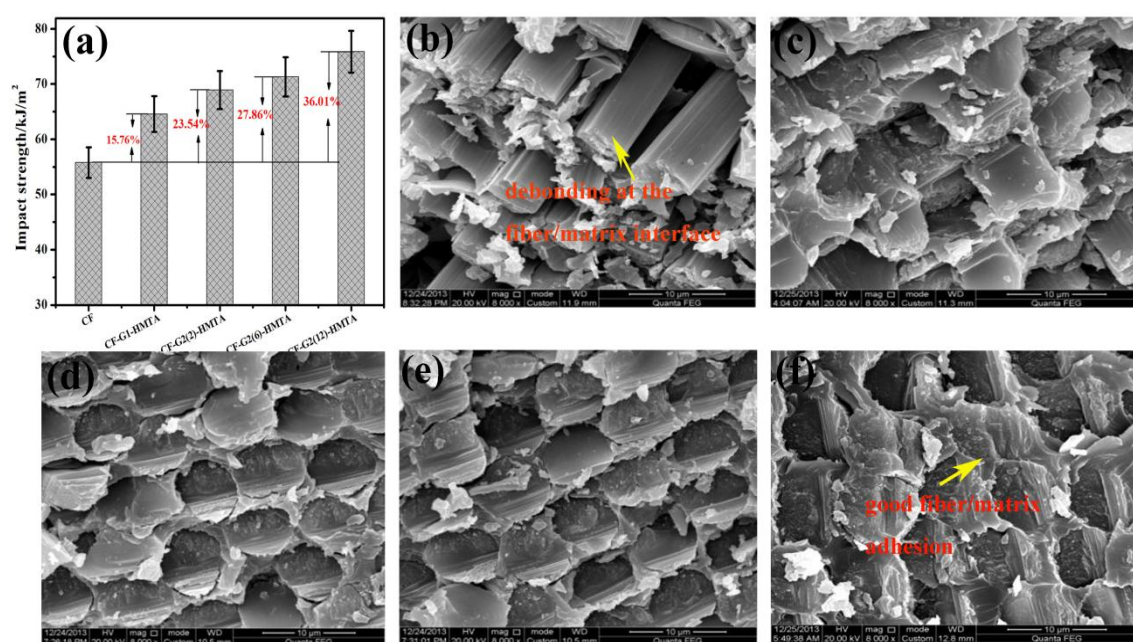


Fig.9 Impact test results of the composites (a) and SEM micrographs of fracture surface of composites (b) untreated CF, (c) CF-G₁- HMTA, (d, e, f) CF-G_{2(n)}- HMTA ($n=2, 6$ and 12)

FESEM observations of the fractured surfaces of the composites are also demonstrated in Fig. 9. For the untreated carbon fiber composites (Fig. 9b), a large number of fibers were pulled out from the matrix, the pulled-out fibers were clean and there were almost no resin fragments adhered on the fiber surface, which indicates the adhesion between fibers and matrix is poor. Compared with Fig. 8b, for the HMTA grafted fiber sample (Fig. 9c), the interfacial adhesion was obviously improved and the number of pulled-out fibers decreased. For the CF-G₂-HMTA (Fig. 9d), the flat fracture surface could be observed, the combination is so close that there is no gap between fiber and resin. And as chain length of alkyl dihalide growth, fracture surface is more flat, but a part of the cross section was covered with the broken fragments of the resin and fiber. This may be because that the introduction of HMTA molecules and the alkyl dihalide of long chain in the interface phase formed a crack network structure during the process of

crack induction and dispersion, which make matrix resin and fiber nearby form a large number of fragments under the action of a large number of cracks. Thus large amounts of energy were consumed and the impact resistance of composite improved with the chain length of alkyl dihalide.

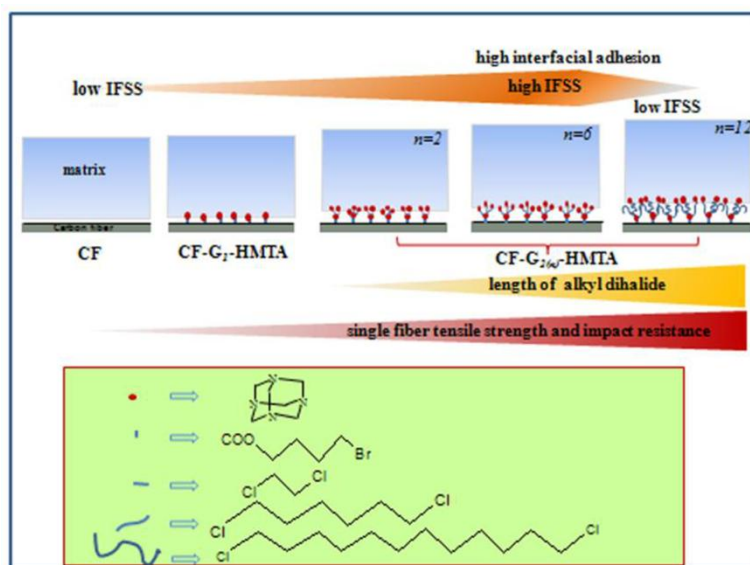


Fig.10 Schematic of the interaction of matrix with CF grafted different chain lengths at the surface.

To summarize, the influence of the different chain lengths on the interfacial adhesion is illustrated in Fig. 10. We can see that the active sites HMTA (indicated by red dot) increases evidently as the dendrimer generation number increases. Compare the schematic illustration of CF-G_{2(n)}-HMTA ($n = 2, 6$ and 12), as the alkyl dihalide chain length increases, the active sites first increases and then decreases, and the entanglements between the chains become more obvious.

Maximum IFSS is expected for a large number of polar groups of HMTA reaction with matrix, combined with strong penetration of the long alkyl dihalide chains into the matrix. But the longest chain length led to a lowering of IFSS due to the decrease of polar groups, so the chemical interaction is also play an important role for the improvement of the interfacial adhesion. Here, we have to consider that the mechanical interlocking is not the only parameter responsible for the interface adhesion. The highest interfacial adhesion can be expected to result from a combination of sufficient chain space, length and polar groups⁵⁷. In addition, dendritic HMTA effectively increased the tensile strength and impact toughness of the composites through increasing the alkyl dihalide chain length. Therefore, according to different applications, a balance of the resulting composite properties among the interfacial adhesion, tensile strength and impact resistance should be considered.

Conclusions

In this study, alkyl dihalide of varying chain lengths in dendritic HMTA were used to investigate the effect of chain length on the interfacial adhesion of CF/epoxy composites. FTIR, Raman and XPS confirmed dendritic HMTA and alkyl dihalide were successful

grafted on the CF surface. AFM results manifested that the roughness of the CF surface increased obviously with alkyl dihalide chain length. The surface energy increased and then decreased with the increase of chain length of alkyl dihalide. IFSS measurements revealed that the longer chain length of the grafted 1, 6-dichlorohexane was crucial for increasing the interfacial adhesion of the CF/epoxy composites, which may be corroborated to the increase in surface energy, polar group and surface roughness. In addition, the tensile strength and impact toughness of the composites enhanced with the alkyl dihalide chain length, the reinforcing and toughening mechanisms were also discussed. These results will provide valuable guidance for the design and manufacture of CF/epoxy composites for different applications.

Acknowledgement

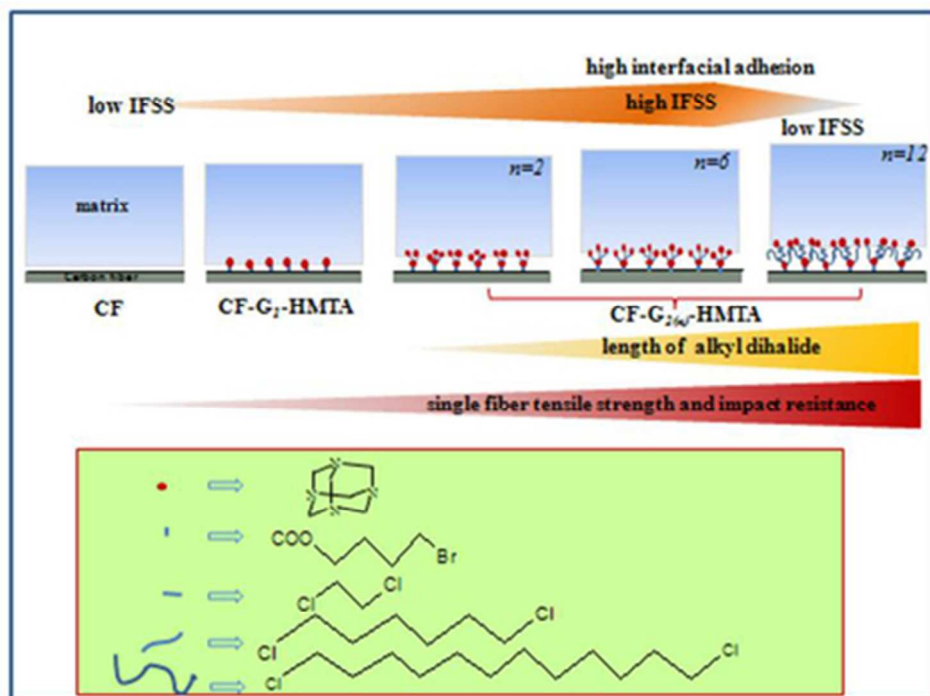
The authors gratefully acknowledge financial support from the National Natural Science Foundation of China (no. 21174034).

References

- 1 M. C. Paiva, C. A. Bernardo and M. Nardin, *Carbon*, 2000, **38**, 1323-1337.
- 2 Q. Y. Peng, X. D. He and Y. B. Li, *J. Mater. Chem.*, 2012, **22**, 5928-5931.
- 3 P. Brondsted, H. Lilholt and A. Lystrup, *Rev. Mater. Res.*, 2005, **35**, 505-538.
- 4 J. George, M. S. Sreekala and S. Thomas, *Polym. Eng. Sci.*, 2001, **41**, 471-1485.
- 5 L.Y. Sun, R. F. Gibson and F. Gordaninejad, *Compos. Sci. Technol.*, 2009, **69**, 2392-2409.
- 6 C. Zhang, J. Hankett and Z. Chen, *ACS Appl. Mater. Interfaces*, 2012, **4**, 3730-3737.
- 7 H. L. Cao, Y. D. Huang and Z. Q. Zhang, *Compos. Sci. Technol.*, 2005, **65**, 1655-1662.
- 8 C. U. Pittman Jr, G. R. He, B. Wu and S. D. Gardner, *Carbon*, 1997, **35**, 317-331.
- 9 M. A. M. Moran, F. W. J. Hattum and J. P. Nunes, *Carbon*, 2005, **43**, 1795-1799.
- 10 Z. W. Xu, Y. D. Huang, C. H. Zhang and L. Liu, *Compos. Sci. Technol.*, 2007, **67**, 3261-3270.
- 11 D. S. Zhang, L. Zhang, L. Y. Shi, C. Fang and H. R. Li, *RSC Nanoscale*, 2013, **5**, 1127-1136.
- 12 D. S. Zhang, L. Zhang, C. Fang, R. H. Gao and L. Y. Shi, *RSC Adv.*, 2013, **3**, 8811-8819.
- 13 J. M. He, Y. D. Huang and L. H. Meng, *J. Appl. Polym. Sci.*, 2009, **112**, 3380-3387.
- 14 K. E. Geckeler, F. Rupp and J. Geis-Gerstorfer, *Adv. Mater.*, 1997, **9**, 513-518.
- 15 C. Kuttner, M. Tebbe and H. Schlaad, *ACS Appl. Mater. Interfaces*, 2012, **4**, 3484-3492.
- 16 L. Chen, Z. Hu, L. Liu and Y.D. Huang, *RSC Adv.*, 2013, **3**, 24664-24670.
- 17 A. Yu, and H. Hu, *Compos. Sci. Technol.*, 2006, **66**, 1190-1197.
- 18 D. Hill, Y. Lin, L. W. Qu and Y. P. Sun, *Macromolecules*, 2005, **38**, 7670-7675.
- 19 B. X. Yang, J. H. Shi and S. H. Goh, *Compos. Sci. Technol.*, 2008, **68**, 2490-2497.
- 20 B. X. Yang, J. H. Shi and S. H. Goh, *Nanotechnology*, 2007, **18**, 1-6.

- 21 X. Q. Zhang, H. B. Xu and X. Y. Fan, *RSC Adv.*, 2014, **4**, 12198-12205.
- 22 A. M. Shanmugaraj and J. H. Bae, *J. Polym. Sci. Chem.*, 2006, **45**, 460-470.
- 23 L. C. Ma, L. H. Meng and Y. D. Huang, *Appl. Surf. Sci.*, 2014, **296**, 61-68.
- 24 L. H. Meng, D. P. Fan and Y. D. Huang, *Appl. Surf. Sci.*, 2012, **261**, 415-421.
- 25 J. L. Yu, L. H. Meng and Y. D. Huang, *Compos: Part B-Eng.*, 2014, **60**, 261-267.
- 26 Y. T. Shieh, G. L. Liu, H. H. Wu and C. C. Lee, *Carbon*, 2007, **45**, 1880-1890.
- 27 X. D. He, F. H. Zhang, R. G. Wang and W. B. Liu, *Carbon*, 2007, **45**, 2559-2563.
- 28 H. M. Huang, I. C. Liu, C. Y. Chang and H. C. TSAI, *J Polym Sci Pol Chem.*, 2004, **42**, 5802-5810.
- 29 H. Q. Peng, L. B. Alemany, J. L. Margrave and V. N. Khabashesku, *J. Am. Chem. Soc.*, 2003, **9**, 125.
- 30 Y. T. Chern, *Macromolecules*, 1995, **28**, 5561-5566.
- 31 M. R. Lockett, J. C. Carlisle, D. V. Le and L. M. Smith, *Langmuir*, 2009, **9**, 5120-5126.
- 32 F. M. Moghaddam and H. Saeidian, *Mat Sci Eng B-Solid*, 2007, **139**, 265-269.
- 33 B. B. Parekh, G. Fanchini, G. Eda and M. Chhowalla. *Appl Phys Lett*, 2007, **90**, 121.
- 34 V. Selvaraj and V. Rajendran. *J. Chem. & Cheml. Sci.*, 2011, **1**, 249-266.
- 35 N. Kaur and D. Kishore. *J Iran Chem Soc*, 2013, **10**, 1193-1228.
- 36 V. I. Levashova and T. P. Mudrik. *Petroleum Chem.*, 2008, **4**, 48.
- 37 G. Şerban, S. Cuc, E. Egri and A. Salvan, *Farmacia*, 2010, **6**, 58.
- 38 S. Shin, J. Jang, S. H. Yoon and I. Mochida, *Carbon*, 1997, **35**, 1739-1743.
- 39 G. X. Chen and H. Shimizu, *Polymer*, 2008, **49**, 943-951.
- 40 J. Liu, Y. Guo and J. Liang, *Acta Mater. Compos. Sin*, 2004, **21**, 40-44. (in Chinese).
- 41 A. Sadezkya, H. Muckenhuberb and H. Grotheb, *Carbon*, 2005, **43**, 1731-1742.
- 42 T. Jawharia, A. Roidb and J. Casadoc, *Carbon*, 1995, **33**, 1561-1565.
- 43 S. Lee, T.R. Kim and M.S. Kim, *Synth. Met.*, 2007, **157**, 644-650.
- 44 G. X. Zhang, S. H. Sun, D. Q. Yang and J. P. Dodelet, *Carbon*, 2008, **46**, 196-205.
- 45 E. Papirer, R. Lacroix, J. B. Donnet and G. Nanse ´, *Carbon*, 1995, **33**, 63-72.
- 46 S. Seal, T. L. Barr, S. Krezoski and D. Petering, *Appl. Surf. Sci.*, 2001, **173**, 339-351.
- 47 J. Li, M. J. Vergne, E. D. Mowles, W. H. Zhong and D. M. Hercules, *Carbon*, 2005, **43**, 2883-2893.
- 48 M. Q. Tran, K. K. C. Ho, G. Kalinka and M. S. P. Shaffer, *Compos. Sci. Technol.*, 2008, **68**, 1766-1776.
- 49 S. L. Gao, E. Mader and S. F. Zhandarov, *Carbon*, 2004, **42**, 515-529.
- 50 J. Duchet, J. P. Chapel and B. Chabert, *Macromolecules*, 1998, **31**, 8264-8272.
- 51 S. R. Jang, R. Vittal and K. J. Kim, *Langmuir*, 2004, **20**, 9807-9810.
- 52 H. Yuan, C. G. Wang, S. Zhang and X. Lin, *Appl. Surf. Sci.*, 2012, **259**, 288-293.
- 53 Q. Y. Peng, Y. B. Li and X. D. He, *Compos. Sci. Technol.*, 2013, **74**, 37-42.
- 54 F. Zhao and Y. D. Huang, *J. Mater. Chem.*, 2011, **21**, 3695-3703.
- 55 Z. W. Xu, L. Chen and Y. D. Huang, *Eur. Polym. J.*, 2008, **44**, 494-503.

- 56 F. Zhao and Y. D. Huang, *Carbon*, 2011, **49**, 2624-2632.
- 57 C. Kuttner, A. Hanisch, H. Schmalz, M. Eder and A. Fery, *ACS Appl. Mater. Interfaces*, 2013, **5**, 2469-2478.



39x30mm (300 x 300 DPI)